PHYSICAL REVIEW B **78**, 064420 (2008)

Magnetic order in the double-layer manganites $(La_{1-z}Pr_z)_{1.2}Sr_{1.8}Mn_2O_7$: Intrinsic properties and role of intergrowth

G. Allodi,* M. Bimbi, and R. De Renzi
Dipartimento di Fisica e Unità CNISM, Università degli Studi di Parma, Viale G. Usberti 7A, I-43100 Parma, Italy

C. Baumann
Institute for Solid State Research, IFW Dresden, P.O. Box 27 01 16, D-01171 Dresden, Germany

M. Apostu
Laboratoire de Physico-Chimie de l'Etat Solide, UMR 8648, Bâtiment 414, Université Paris-Sud, 91405 Orsay, France and Department of Physical, Theoretical and Materials Chemistry, Faculty of Chemistry, "Alexandru Ioan Cuza" University, 11 Carol I Boulevard, 700506 Iasi, Romania

R. Suryanarayanan and A. Revcolevschi
Laboratoire de Physico-Chimie de l'Etat Solide, UMR 8648, Bâtiment 414, Université Paris-Sud, 91405 Orsay, France
(Received 30 May 2008; published 21 August 2008)

We report on an investigation of the double-layer manganite series $(La_{1-z}Pr_z)_{1.2}Sr_{1.8}Mn_2O_7$ $(0 \leq z \leq 1)$, carried out on single crystals by means of both macroscopic magnetometry and local probes of magnetism [muon-spin rotation (μSR), ^{55}Mn NMR]. Muons and NMR demonstrate an antiferromagnetically ordered ground state at nonferromagnetic compositions ($z \geq 0.6$), while more moderate Pr substitutions ($0.2 \leq z \leq 0.4$) induce a spin reorientation transition within the ferromagnetic phase. A large magnetic susceptibility is detected at $T_{C,N} < T < 250$ K at all compositions. From ^{55}Mn NMR spectroscopy, such a response is unambiguously assigned to the intergrowth of a ferromagnetic pseudocubic phase $(La_{1-z}Pr_z)_{1-x}Sr_xMnO_3$, with an overall volume fraction estimated as 0.5%–0.7% from magnetometry. Evidence is provided for the coupling of the magnetic moments of these inclusions with the magnetic moments of the surrounding $(La_{1-z}Pr_z)_{1.2}Sr_{1.8}Mn_2O_7$ phase, as in the case of finely dispersed impurities. We argue that the ubiquitous intergrowth phase may play a role in the marked first-order character of the magnetic transition and the metamagnetic properties above T_c reported for double-layer manganites.

DOI: 10.1103/PhysRevB.78.064420 PACS number(s): 74.62.Dh, 75.47.Lx, 76.75.+i, 76.60.−k

I. INTRODUCTION

In the last decade, double-layer strontium manganites $La_{2-2x}Sr_{1+2x}Mn_2O_7$ have attracted the interest of the colossal magnetoresistance (CMR) community due to a magnetoresistive effect that is even larger than in the pseudocubic compounds $La_{1-x}Sr_xMnO_3$ and for their peculiar anisotropic magnetotransport properties. These systems are the $n=2$ members of the Ruddlesden-Popper (R-P) series $La_{n(1-x)}Sr_{1+nx}Mn_nO_{3n+1}$, constituted by blocks of two adjacent magnetic MnO_2 planes, decoupled from each other by a rocksaltlike block of nonmagnetic oxide (La,Sr)O. At optimum doping ($x=0.4$), the material is a quasi-two-dimensional ferromagnetic metal (FMM) with a reported Curie temperature $T_C \approx 125$ K (Ref. 1) and a highly anisotropic electrical conductivity σ (2 orders of magnitude larger in the *ab* plane than along the *c* axis).[1,2] In some sense, these compounds may be viewed as a natural kind of FMM-oxide multilayers and hence prototype systems for the study of the physics of spin-polarized electrons in heterostructures, which is the clue for the production of spintronic devices.

As for their pseudocubic counterparts, the electronic and magnetic states of these materials result from the competition between different interactions, comparable in energy scale. While Zener's double exchange (DE) dominates in the FMM state ($0.32 \leq x \leq 0.45$), electronic correlations drive the system through a number of different insulating phases with distinct types of magnetic, charge, and orbital order as a function of temperature and hole doping x, leading to a very complex phase diagram.[3] Because of the reduced dimensionality, however, the DE term is less effective in the double-layered compounds, as indicated by their strongly diminished Curie temperatures ($T_C=125$ and 370 K in $La_{2-2x}Sr_{1+2x}Mn_2O_7$ and $La_{1-x}Sr_xMnO_3$, respectively, around optimal doping $x=3/8$). Further DE energy reduction may arise from cation size mismatch when different alkali-earth metals and rare earths are substituted. The small ionic radius of Pr^{3+} induces distortions and tilting of the MnO_6 octahedra, which depress the hopping term both by directly reducing the overlap of the Mn and O orbitals and by altering the relative populations of the e_g orbitals.[4] As a result, the FMM phase may become unstable, and the systems exhibit metal-insulator (MI) transitions.

The isoelectronic series $(La_{1-z}Pr_z)_{1.2}Sr_{1.8}Mn_2O_7$ shows indeed an insulating nonferromagnetic ground state for $z > 0.5$. Nevertheless, the FMM phase still exists at these compositions as a metastable one, into which the system can be driven by applying a magnetic field on the order of a few teslas at low temperature or by cooling the sample in an even smaller applied field.[5] The former process is actually a field-induced first-order MI transition, and the corresponding drop in electrical resistivity may be viewed as another kind of

CMR. The system displays peculiar thermal and magnetic hysteresis effects, and the FMM state survives even after removal of the magnetic field.[6]

While the MI transition has been subject of vast investigation and is well understood,[7,8] magnetism in the non-FMM phases of this series has been debated for long time. No spontaneous magnetic order has ever been demonstrated at $z>0.5$ in the so-called virgin state (zero field, zero-field cooled) at low temperature. Hence the systems have been assigned to a spin-glass state.[4] Moreover, the nature of the paramagnetic phase itself in double-layer manganites is the subject of a controversy reaching well beyond the issue of La-Pr substitution. These systems exhibit in fact enhanced magnetic susceptibility well above the highest known T_C of a double-layer manganite, up to close to room temperature. At the same temperatures, angle-resolved photoelectron spectroscopy (ARPES) recently showed evidence in $La_{1.24}Sr_{1.76}Mn_2O_7$ for a locally metallic phase in a globally insulating state.[9] Although the possible presence of spurious FMM inclusions in the sample has been considered in many papers, there is however general disagreement about their role in the anomalous responses detected in the paramagnetic phase. According to some authors, such responses are essentially intrinsic spin and electronic properties of the double-layer material,[9–11] while they are mostly due to the intergrowth of a secondary FMM phase for some other.[12]

In this paper, we address the issue of the magnetic state of La-Pr double-layer manganites by means of local probes of magnetism, namely, muon-spin rotation (μSR) and ^{55}Mn NMR. Implanted muons are sensitive probes of local magnetic fields in the matter, suited to investigation of the magnetic structure even in the case of short-range order or dilute magnetic clusters, where probes in the reciprocal space cannot detect any magnetic Bragg peak. In addition, ^{55}Mn NMR in zero external field provides a determination of the spontaneous hyperfine fields at ^{55}Mn nuclei, which constitutes a probe of both magnetic order and the electronic state of the Mn ions. The investigation is complemented by magnetization and magnetic-susceptibility measurements. By combining these techniques, we demonstrate that the $z>0.5$ compositions display short-range antiferromagnetic order below a Néel temperature $T_N \approx 60$ K, while any ferromagnetic response above that temperature is to be assigned to pseudocubic FMM inclusions, on the order of 1% of sample volume.

The paper is organized as follows: Section II provides a brief description of sample preparation and the experimental methods, as well as the essential guidelines to the NMR technique applied to the study of manganites. In Sec. III A we describe the μSR results on the changes in magnetic structure across the phase diagram. In Sec. III B we present evidence for ferromagnetic intergrowths from magnetometry and susceptometry. The electronic nature of the intergrowths and their peculiar coupling to the bilayer manganite domains are further elucidated by ^{55}Mn NMR in Sec. III C. Results are discussed in Sec. IV.

II. EXPERIMENT

A. Samples

The single crystals were grown through the floating-zone method by using an image furnace, melting sintered rods of polycrystalline materials of the same nominal compositions obtained by standard solid-state reaction. For ^{55}Mn NMR on unsubstituted $La_{1.2}Sr_{1.8}Mn_2O_7$ at low temperature, however, we employed the original powder material instead of the final single crystal due to the small penetration depth of radio frequency (rf) in a metal, making a bulk conductive sample opaque to the driving rf field. A subset of these crystals was subjected to the investigations reported in Refs. 6–8, 10, and 13. Preliminary magnetic characterization by macroscopic dc magnetization measurements in a field of 10 mT confirmed ferromagnetic (FM) order at compositions $z \leq 0.4$, with Curie temperatures decreasing from ≈ 110 K in the Pr-free compound down to $T_C \approx 60$ K at $z=0.4$, and a non-FM state at $z \geq 0.6$.[13]

B. Magnetometry

Measurements were carried out by means of a Quantum Design MPMS-XL superconducting quantum interference device (SQUID), employed either as a dc magnetometer or as an ac susceptometer in zero-bias field. Magnetic ac susceptibility was also measured vs temperature in the rf domain from the increase in inductance of a small coil ($L_0 \approx 200$ nH in air) wound around the sample and placed in a liquid-nitrogen cryostat. The coil was driven by a rf field of ≈ 0.01 Oe at a frequency of ≈ 50 MHz by a Hewlett-Packard 4191A impedance meter, to which it was connected by a $\lambda/2$ coaxial cable for the working frequency. The inductance L is related to the rf volume magnetic susceptibility χ_{rf} by

$$(L-L_0)/L_0 = f 4\pi\chi_{\mathrm{rf}}/(1+N4\pi\chi_{\mathrm{rf}}), \tag{1}$$

where N and f are the demagnetization and filling factors of the sample, respectively. In the case of a bulk conductive sample, a significant diamagnetic contribution to χ_{rf} may also arise from eddy currents. This rf method is therefore intended as a qualitative characterization, sensitive only to large FM components.

C. ^{55}Mn NMR in manganites

Nuclear-magnetic-resonance experiments were performed by means of a home-built phase-coherent spectrometer,[14] using an Oxford EXA field-swept cold-bore cryomagnet as a sample environment. Spectra were recorded point by point at frequency steps of 1 MHz by a standard P-τ-P spin-echo sequence, with delays τ of 3–5 μs and equal rf pulses P of 0.5–2 μs with intensity optimized for maximum signal. NMR signals from antiferromagnetic (AF) phases, characterized by a small rf enhancement factor (see below), were detected by a tuned probe head, while the strongly enhanced signals from FM phases could be detected by a nonresonant circuit (a small coil terminated onto 50 Ω) with a fully automated procedure.

The ^{55}Mn nuclear probe is coupled to the electronic Mn moments by the hyperfine interaction, of the form

$$\mathcal{H} = \hbar\,{}^{55}\gamma g \mu_B \boldsymbol{S}\cdot\mathcal{A}\cdot\boldsymbol{I}, \tag{2}$$

giving rise to a spontaneous magnetic field $\boldsymbol{B}_{\mathrm{hf}} = g\mu_B\mathcal{A}\langle\boldsymbol{S}\rangle$ at the nuclei in the magnetically ordered state of the material.

Here $\boldsymbol{S}$ and $\boldsymbol{I}$ are the electron and nuclear spins, g is the Landé factor, μ_B is the Bohr magneton, $^{55}\gamma$ is the nuclear gyromagnetic ratio, and $\mathcal{A}$ is the on-site hyperfine coupling tensor. All other terms, such as transferred contributions and dipolar fields from nearest-neighbor ions, have been neglected in Eq. (2) since they are much smaller.

From Eq. (2), the spontaneous resonance frequency, proportional to the hyperfine field, essentially depends on the on-site electronic spin, as well as on the valence of the magnetic ions and the metallic vs insulating electronic state. Experimentally, the isotropic component of the hyperfine coupling constant (the Fermi contact term) exhibits a value of $\mathcal{A}_{\rm iso} \approx 10$ T/μ_B throughout the iron transition-metal series, approximately independent of the ionic species.[15] In the case of manganites, $\mathcal{A}_{\rm iso}$ would give rise to resonance frequencies of approximately 300 and 400 MHz for Mn^{4+} ($S=3/2$) and Mn^{3+} ($S=2$), respectively.

The hyperfine field of Mn^{3+}, however, also exhibits a sizable pseudodipolar component $g\mu_B \mathcal{A}_{\rm dip} \cdot \boldsymbol{S}$ on the order of 100 kOe, while the anisotropic coupling tensor $\mathcal{A}_{\rm dip}$ vanishes for the octahedral symmetric Mn^{4+} ion. As a consequence of this anisotropic coupling term, the resonance frequency of ^{55}Mn in Mn^{3+} may lie anywhere in the 250–500 MHz frequency range, depending on the orientation of the electronic spin relative to the ionic symmetry axis.[16] In the presence of many magnetically nonequivalent sites, the resonance of ^{55}Mn in Mn^{3+} may be split into a number of satellite lines, as it was actually found in insulating low-doped $La_{1-x}Sr_xMnO_3$.[17] At increased structural or magnetic disorder, $\mathcal{A}_{\rm dip}$ of Mn^{3+} may simply contribute to a huge inhomogeneous linewidth, while the resonance of ^{55}Mn in Mn^{4+} are comparatively much sharper. In the metallic state of pseudocubic $La_{1-x}Sr_xMnO_3$, however, individual 3+ and 4+ ions are replaced by a single Mn mixed valence of $3+x$, while the pseudodipolar coupling term is averaged out by fast electronic motion. As a consequence, the broad and complex NMR spectrum typical of the insulating compositions collapses into a single motionally narrowed line in the metallic state.

Information about the type of magnetic order, ferro- or antiferromagnetic, can be obtained by NMR from the so-called radio-frequency enhancement, consisting of an amplification of the effective rf field at the nucleus, due to the hyperfine coupling between nuclear and electronic spins. An applied rf field couples to the magnetization of a magnetic material and tilts its electronic moments, thus inducing a modulation of the hyperfine field at the nucleus at the same frequency.[18,19] Since the hyperfine field is on the order of several teslas, a small rf perturbation usually gives rise to a large modulation of $B_{\rm hf}$ at the same frequency. Hence, if H_1 is the rf field applied in the sample coil, the effective rf field driving the resonance at the nucleus is enhanced by a factor $\eta > 1$, $H_1^{\rm eff} = \eta H_1$. As compared to NMR of the same nucleus in a nonmagnetic material, nuclear resonance can therefore be excited by reduced rf power. The same amplification mechanism holds for the NMR signal induced in the pick-up coil: $A \propto \eta N$, where A is the signal amplitude and N is the number of resonating nuclei.

The rf enhancement depends on the local magnetic structure and on the effective magnetic anisotropy. Clearly, η is larger in ferromagnets because of their larger net magnetization coupling to the external rf field. Two enhancement mechanisms may be distinguished in a ferromagnet: The applied rf field may displace the domain walls, or it may rotate the magnetization in the bulk of domains. The former comes into play for nuclei within domain walls and is generally the dominant mechanism in zero field, where it may give rise to values of $\eta \approx 10^3 - 10^4$, while it vanishes in an applied static field above the saturation value. The latter is usually less effective by 1–2 orders of magnitude, and it is present both in zero and in an applied field. In special cases (e.g., uniaxial anisotropy and H_1 perpendicular to the easy axis), straightforward calculation yields a domain enhancement factor $\eta_d \propto H_{\rm anis}^{-1}$, where $H_{\rm anis}$ is the anisotropy field, while such a relation may be taken only as a qualitative one for the domain-wall enhancement η_w, whose actual dependence is much more complicated.

D. μSR experiments

The experiments were performed at Paul Scherrer Institut (Villigen, CH) on the GPS spectrometer in the spin-rotator (SR) setup. The asymmetry of the muon decay, $A(t)$, is directly proportional to the time dependent muon-spin projection along the axis joining a detector pair at the opposite sides of the sample, which reveals the spin precession around the local field.[20] With the SR the initial muon polarization is rotated from the beam direction ($\hat{x}$ axis) by $\approx 47°$ toward the vertical axis ($\hat{y}$), while emitted positrons were detected by two detector pairs along $\hat{x}$ and $\hat{y}$. This allowed simultaneous detection of the muon-spin projections parallel and perpendicular to c. The crystals were mounted with the c axis parallel to either $\hat{x}$ or $\hat{y}$, as deemed appropriate.

In transition-metal oxides muons stop at few (typically one or two) distinct interstitial sites. The muon spin is coupled to the electronic Mn moments by dipolar and hyperfine interactions, providing a different local magnetic field $\boldsymbol{H}_{\mu j}$ at each distinct site. Depending on its orientation, each local field gives rise to precessing and to longitudinal components of the muon spin, revealed respectively by damped oscillations and purely relaxing terms in the muon asymmetry. The muon polarization $P_\mu(t)$ may be fitted as

$$P_\mu(t) = \frac{A(t)}{A_0} = \left[a_1 e^{-t/T_1} + \sum_j a_{2j} e^{-t/T_{2j}} \cos \omega_j t \right], \qquad (3)$$

where A_0 is the total calibrated asymmetry for the GPS SR setup, $\omega_j = \gamma_m u H_{\mu j}$ are the muon precession frequencies, $\gamma_\mu / 2\pi = 135.54$ MHz/T is the muon gyromagnetic ratio, a_1, T_1 and a_{2j}, T_{2j} are the muon amplitudes and their respective relaxation times for the longitudinal and precessing components, respectively. Since precessing components are distinguished by their frequencies, whereas longitudinal components are not, only a cumulative term may be determined experimentally for the latter.

III. EXPERIMENTAL RESULTS

We report separately the results obtained by the different techniques, starting from μSR, then magnetometry, and finally NMR.

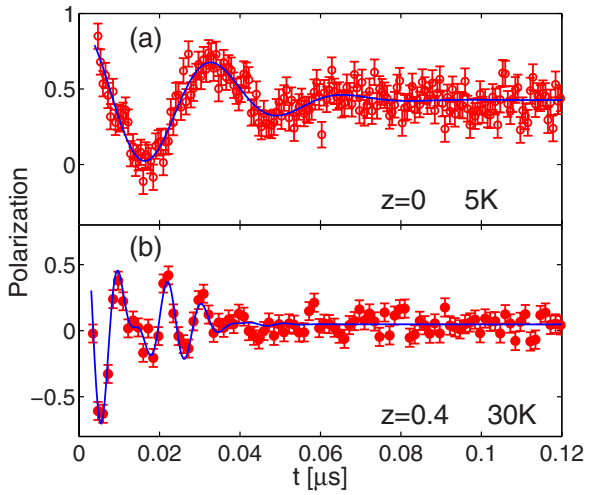

FIG. 1. (Color online) Time evolution of muon-spin polarization along the c axis in (a) $La_{1.2}Sr_{1.8}Mn_2O_7$ and (b) $(La_{0.6}Pr_{0.4})_{1.2}Sr_{1.8}Mn_2O_7$ at $T \ll T_C$.

A. μSR results

Precessing patterns are detected in the ordered phase at all FMM compositions, up to $z=0.4$. Figure 1 shows the low-temperature time dependent polarization at the two extremes of this range, with a best fit to Eq. (3). The analysis of frequencies and fractions for the different compositions, summarized below, reveal two distinct long-range-order magnetic structures at these two extremes and a third form of short-range magnetic order for higher Pr content. Relaxations in the paramagnetic phase, described separately, identify an additional contribution for all samples.

1. $z=0$

In the unsubstituted compound we detected a single precession component [Fig. 1(a)] with an internal field of 220 mT (29.6 MHz in frequency units) at $T=5$ K, in close agreement with the value reported by Coldea *et al.*[21] for the same nominal material. Such a field is significantly smaller than the typical values reported for pseudocubic[22,23] and single-layer[24] manganites (on the order of 6–10 kG). The precession frequency and the longitudinal amplitudes a_1 for the detector pair perpendicular to the c axis are plotted vs temperature in Fig. 2(a). In the magnetically ordered state, we detected a finite longitudinal amplitude also for the spin projection $\parallel c$ (data not shown), indicating that the direction of the internal field $\boldsymbol{H}_\mu$ is tilted relative to the crystal axes.

The recovery of the full longitudinal amplitude, denoting the transition to the paramagnetic phase, may be fitted by a Gaussian distribution of Curie temperatures with a rather low average $T_C=105\pm3$ K and width $\Delta T_C=8$ K [dotted line in Fig. 2(a)]. Although the distribution of transition temperature indicates a residual inhomogeneity, the internal field H_μ vanishes following the order parameter as $(T-T_C)^\beta$, as in regular second-order transitions. This behavior is markedly different from any previously reported in the literature for these metallic compositions. For instance, Ref. 25 on a nominally similar $La_{1.2}Sr_{1.8}Mn_2O_7$ determined $T_C=126$ K and a "truncated" first-order-like transition, common to all metallic manganites (with the exception of the large-bandwidth compound $La_{1-x}Sr_xMnO_3$). In such transitions the order parameter remains finite for $T \to T_c$, while the volume of the ordered phase shrinks as the transition temperature is approached.[26,27]

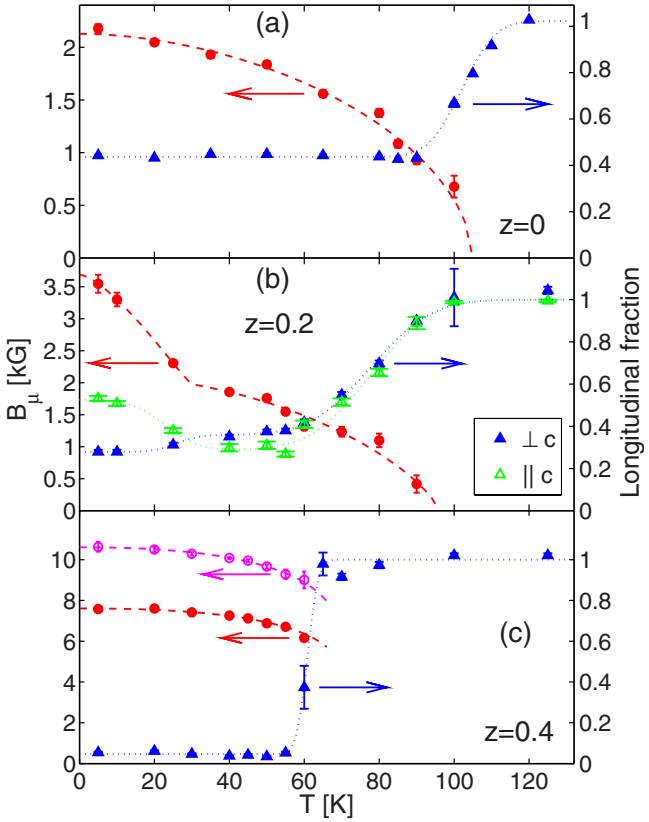

FIG. 2. (Color online) Muon spontaneous fields (bullets) and longitudinal amplitudes (triangles) as a function of temperature, in the (a) $z=0$, (b) $z=0.2$, and (c) $z=0.4$ samples. The open and filled triangles denote amplitudes along and perpendicular to the c axis, respectively. The dashed lines are guides to the eye (dotted lines; see text).

2. $z=0.4$

Two precessing components could be resolved in the case of $(La_{0.6}Pr_{0.4})_{1.2}Sr_{1.8}Mn_2O_7$ [Fig. 1(b)], with much higher internal fields of 7.6 and 10.6 kG at 5 K [Fig. 2(c)]. Their total precessing amplitude at $T \ll T_C$ is close to 100% for the detector pair perpendicular to the c axis and it is negligibly small for that $\parallel c$, while the opposite occurs for the longitudinal amplitude. This demonstrates that the internal fields at both muon sites are collinear with c within the accuracy of sample orientation ($\pm5°$).

This markedly different behavior of both precession amplitudes and frequencies with respect to the unsubstituted compound arises from the spin reorientation induced by La-Pr substitution, reported by Vasil'ev *et al.*,[28] who detected an easy magnetization axis perpendicular to c in praseodymium-free $La_{2-2x}Sr_{1+2x}Mn_2O_7$ and parallel to the c axis at $z=0.4$. Such a reorientation strongly affects the magnitude of the local field due to the anisotropy of the muon-

electron interaction (essentially the dipolar coupling between the muon and electronic spins). The temperature dependence of the longitudinal amplitude [Fig. 2(c)] reveals a rather sharp magnetic transition at $T_C=60\pm1$ K. In contrast to the $z=0$ case, this transition shows a strong first-order character, as witnessed by the high value of the internal fields at both muon sites just before the transition, $H_{\mu j}(T_C)/H_{\mu j}(0)\approx0.85$.

3. $z=0.2$

In the ordered phase of the intermediate compound $(La_{0.8}Pr_{0.2})_{1.2}Sr_{1.8}Mn_2O_7$, muons precess at the same single frequency as in the unsubstituted material except at very low temperature [Fig. 2(b)]. In the 30–60 K interval, the μSR spectra of this and the $z=0$ samples are closely similar, in particular the values of $H_\mu(T)$ and the relative weights of the longitudinal and transverse amplitude A_1/A_2 coincide within experimental errors. In the $z=0.2$ sample, however, the recovery of the full longitudinal asymmetry takes place continuously on warming from 60 to 90 K, which indicates an even broader distribution of T_C. Moreover, the precession signal shows a clear anomaly at $T<20$ K, consisting in an upturn of both the internal field and the precession amplitude perpendicular to c, along with a complementary reduction in the longitudinal amplitude for the same detector pair. The precession linewidth increases as well at $T\to0$, which might mask the presence of two distinct though poorly resolved precession frequencies, as in the case of $z=0.4$. Following the discussion above, such a low-temperature dependence of the magnitude and direction of the local field $\boldsymbol{H}_\mu$ is indicative of a partial spin reorientation, apparently governed by an energy scale on the order of a few tens of kelvins at this composition.

4. $z\geq0.6$

The appearance of large static internal fields in the non-FMM compounds, originating from a nonfluctuating component of the electronic spins, is proved by the drop in the longitudinal amplitudes below a magnetic transition temperature $T_N=55\pm5$ K, nearly independent of z [Fig. 3(a)]. No spontaneous muon precession signal could be detected at these compositions after zero-field cooling. This indicates a very broad distribution of large internal fields, leading to an exceedingly fast depolarization of the transverse muon signal, which is already relaxed at early times. In Fig. 3(a), comparison between the longitudinal signals detected parallel and perpendicular to the c axis reveals however that the local field at the muon site $\boldsymbol{H}_\mu$, though not collinear to the crystal axes, has a dominant component along c. Such a correlation of the internal field direction with the crystal lattice rules out a spin-glass state. Moreover, in conjunction with the small macroscopic moment,[6] it demonstrates a low-temperature antiferromagnetic order in the samples, although one of short-range character.

5. Relaxations

The zero-field polarization of all the crystals in our series exhibits exponential relaxations with sizable rates in the paramagnetic (PM) state, up to temperatures on the order of

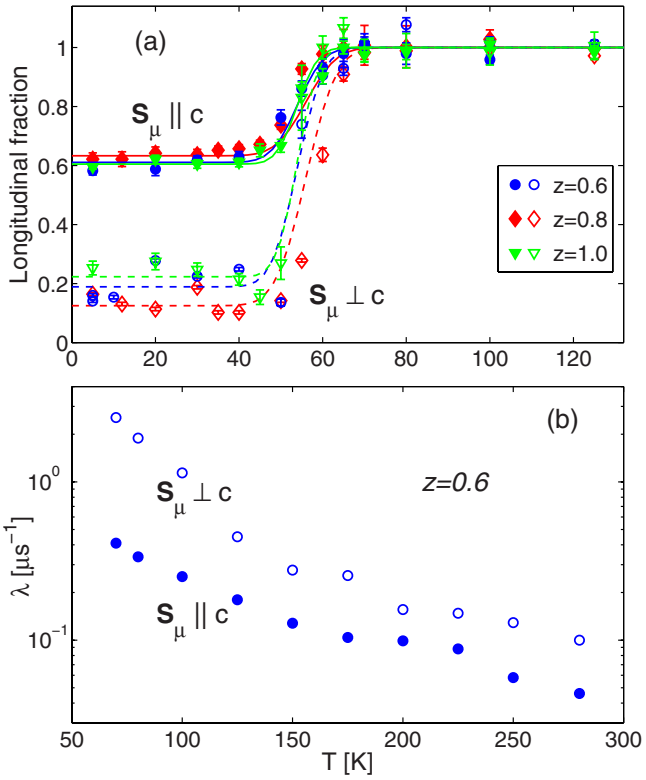

FIG. 3. (Color online) (a) Muon longitudinal amplitudes as a function of T at AF compositions parallel (filled symbols) and perpendicular to the c axis (open symbols). (b) Longitudinal relaxations in $(La_{0.4}Pr_{0.6})_{1.2}Sr_{1.8}Mn_2O_7$ at $T>T_N$ for the two muon-spin components.

200 K, well above $T_{C,N}$. We refer to these rates by using the symbol λ, to explicitly avoid labeling them as longitudinal (T_1^{-1}) or transverse (T_2^{-1}). Their magnitude, $\lambda\approx1$ μs^{-1} at 100 K, clearly proves their electronic origin, since random dipolar fields by static nuclei determine Gaussian relaxation with much smaller rates, never exceeding ≈0.1 μs^{-1} in any known manganite compound.[24,29] Strong dynamic relaxations in the paramagnetic regime may indeed originate from the critical slowing down of fluctuations. However they are usually confined to a narrow temperature interval just above $T_{C,N}$, contrary to our observations.

Figure 3(b) shows the temperature dependence of λ measured on a representative sample ($z=0.6$) in zero external field (ZF), in the PM phase. Two different rates are measured simultaneously in the SR setup (see Sec. II D), equivalent to independent measurements in longitudinal detectors (i.e., *along* the initial muon-spin direction $\boldsymbol{S}_\mu^0$) with the crystal c axis aligned respectively parallel and perpendicular to the detector axis, hence to $\boldsymbol{S}_\mu^0$. A marked relaxation anisotropy is apparent, with the ZF depolarization rate of the muon-spin component perpendicular to the c axis exceeding that of the parallel component by nearly 1 order of magnitude, up to well above $4T_N$. Also the unsubstituted crystal shows a qualitatively similar behavior above its transition temperature, albeit with slightly reduced rates.

If this unusual ZF relaxation were due to static magnetic moments, the value of the rate, 0.4 $\mu s^{-1}\leq\lambda\leq3$ μs^{-1}, would be directly proportional to the static internal local

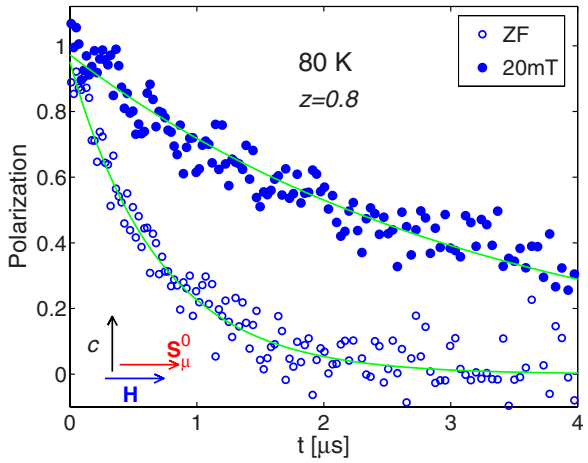

FIG. 4. (Color online) $(La_{0.2}Pr_{0.8})_{1.2}Sr_{1.8}Mn_2O_7$: muon-spin polarization vs time at 80 K for initial muon spin $\boldsymbol{S}_\mu^0$ perpendicular to the c axis in zero field (open symbols) and external field $\mu_o H = 20$ mT, $\boldsymbol{H} \| \boldsymbol{S}_\mu^0$ (filled symbols).

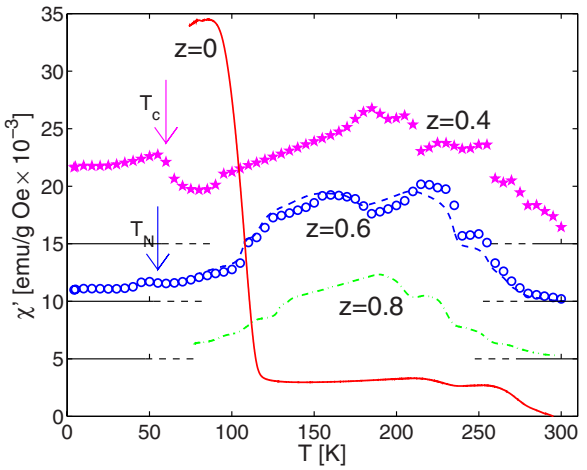

FIG. 5. (Color online) ac susceptibility χ' ($H_{ac} \perp c$ axis) as a function of temperature, measured either by SQUID at acoustic frequency (markers) or by the rf method described in the text (lines). For clarity, data are plotted with constant vertical offsets.

fields, $0.4\ \text{mT} \leq B_{\mu,s} \leq 4\ \text{mT}$. Conversely, similar rates could be due to much larger instantaneous internal fields $B_\mu \gg B_{\mu,s}$, fluctuating with reciprocal correlation times τ^{-1} larger than their Larmor frequencies $2\pi\gamma_\mu B_\mu$ (dynamical rates scale with $B_\mu^2 \tau$). In order to clarify this issue, we measured the muon polarization in a magnetic field $\mu_0 H > B_{\mu,s}$, which is expected to influence the rates in the first case but not in the second.

The time dependent polarizations in zero and in a longitudinal field of 20 mT are compared in Fig. 4 for another sample ($z=0.8$, but the behavior is generic) at 80 K $> T_N$ and with the initial muon spin $\boldsymbol{S}_\mu^0$ perpendicular to the c axis. It is apparent that the application of a moderate longitudinal field (i.e., parallel to both $\boldsymbol{S}_\mu^0$ and the detectors) *quenches* significantly the strong ZF polarization decay observed in this geometry. This clearly identifies the presence of a dominant static contribution at $T > T_{C,N}$; i.e., these zero-field relaxations are essentially due to incoherent precessions in random static fields. Only transverse static fields $\boldsymbol{B}_{\mu,s} \perp \boldsymbol{S}_\mu^0$ contribute to such a mechanism; longitudinal ones, on the contrary, do not depolarize the muon spin. Therefore, the anisotropy in the ZF decay rates, $\lambda_{ab} \gg \lambda_c$, witnesses an anisotropic distribution of $\boldsymbol{B}_{\mu,s}$ peaked along the c axis. We remark that similar anisotropic relaxations were reported in double-layer manganites by Heffner *et al.*,[30] who however overlooked their static character.

B. Magnetic response

We performed SQUID susceptibility measurements on the two samples closer to the MI phase boundary, namely, $z=0.4$ and $z=0.6$, in an ac field of 0.1 Oe at 131 Hz applied in the ab plane and dc field zeroed within a fraction of the earth's magnetic field. In the $z=0.4$ sample, the onset of FM order below $T_C \approx 60$ K is marked by the rise in χ', while in $z=0.6$ the magnetic transition shows up as a shallow bump at $T_N \approx 55$ K (Fig. 5). Such low-temperature features, however, are overwhelmed at both FM and AF compositions by a huge response from 270 down to 80 K, exhibiting a broad peak structure between 150 and 200 K, which drops on approaching $T_{C,N}$. This anomalous response in the PM phase is suppressed by a bias dc field on the order of a few tens of oersteds. Static magnetization curves $M(T)$ in $H_{dc} \geq 100$ Oe (not shown) closely reproduced those published in Ref. 13.

Radio-frequency measurements in the 77–300 K temperature interval and zero dc field yield $L(T) - L_0$ data proportional to χ_{ac} as measured by SQUID at acoustic frequencies.[39] In $La_{1.2}Sr_{1.8}Mn_2O_7$, the rf data provided an independent estimate of the Curie point, which is determined as $T_C = 105 \pm 3$ K from the inflection point of $L(T)$, in agreement with our μSR data. In this as well as in the substituted samples, the rf response also displays anomalous paramagnetic peaks above $T_{C,N}$, equivalent to the SQUID ones. Such peaks are more intense in the Pr-substituted samples than in $La_{1.2}Sr_{1.8}Mn_2O_7$, and they are suppressed by a small dc magnetic field such as those in χ_{ac} at 131 Hz.

The insensitivity of the anomalous paramagnetic response to the driving frequency, up to the rf domain, demonstrates the absence of significant dissipation and rules out, for instance, a spin-glass state. Indeed, dc magnetization measurements reveal a net moment in the PM phase which rather points to the presence of FM inclusions in the samples. Figure 6 plots typical $M(H)$ curves at $T > T_{C,N}$, showing an initial steep growth of the magnetization M, followed by a much reduced linear increase at higher fields. The change in slope takes place at a few tens of oersteds, roughly the same field value required to suppress the anomalous high-temperature contribution to χ'_{ac}. Clearly, the initial growth corresponds to the low-field saturation of the magnetic moments of the inclusions, while the linear behavior at higher fields is the genuine PM response of the double-layer manganite. These FM impurities obviously coincide with the intergrowths suggested by μSR. From the intercept of the linear high-field behavior at $H=0$, $M_0 \approx 0.4(1)$ and $0.6(1)$ emu/g, respectively, in the Pr-free and Pr-substituted compounds, we estimate the corresponding intergrowth fractions

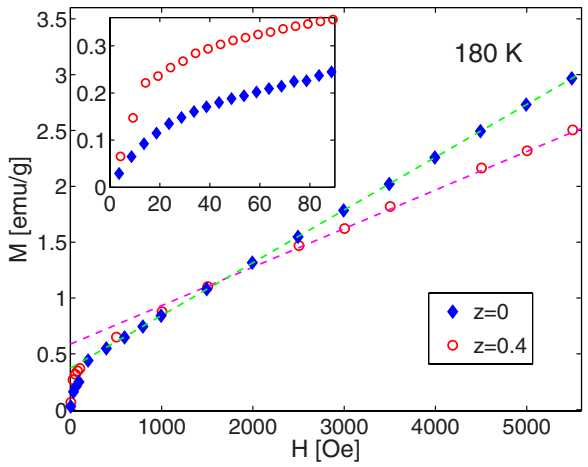

FIG. 6. (Color online) Magnetic moment vs applied field ($H \perp c$ axis) at 180 K, at $z=0$ and $z=0.4$. Inset: blowup at small fields.

to be 0.5(1) % and 0.7(1) % of the crystal volume, respectively.

The small saturation field of these clusters, along with the absence of detectable magnetic hysteresis, demonstrate their soft magnetism at temperatures which are well above the $T_{C,N}$ of the pure double-layer manganite. A drop in the ac susceptibility takes place below 120–150 K. This is evident in the AF members, where $\chi'(T)$ reaches a minimum just below T_N. It is still distinguishable in the $z=0.4$ sample, whereas it is masked by the double-layer ferromagnetic response in the $z=0$ sample. The strong decrease in the high-temperature $\chi'(T)$ indicates an increase in the magnetic anisotropy of the intergrowth on cooling. Its occurrence on approaching T_N suggests that the magnetic hardening of the FM clusters might be induced by the AF order in the host matrix via their exchange coupling with the double-layer manganite.

C. Zero-field ^{55}Mn NMR

In the nonferromagnetic samples $z \geq 0.6$, two distinct kinds of ^{55}Mn NMR signals were detected in zero field (ZF-NMR) at low temperature, whose spectra are shown in Fig. 7(a) for a representative sample ($z=0.8$). The narrower single peak at 377 MHz, characteristic of a pseudocubic DE phase, was excited with a sizable enhancement $\eta \approx 300$, slightly smaller than the typical values previously reported for the zero-field ^{55}Mn signal in CMR manganites,[17,31] while the broader two-peak spectrum in the 270–450 MHz range was detected with a much smaller enhancement value of $\eta \approx 10$. The amplitudes integrated over the spectrum of the two signals are in the ratio 1:1.3, respectively. Since however the ratio of their enhancement factors is ≈ 30, the actual fraction of nuclei from which the former signal originates is estimated as $\approx 2 \pm 1\%$,[40] and therefore the single-peak spectrum is due to a minority phase.

The minority phase is both ferromagnetic and metallic, as indicated by the large rf enhancement and its motionally narrowed single-peak spectrum, respectively. The proper spectrum of insulating $(La_{1-z}Pr_z)_{1.2}Sr_{1.8}Mn_2O_7$ is the broad two-peak one and the presence of a zero-field resonance signal, hence well-defined $[\overline{(\Delta B_{hf}^2)}^{1/2}/\overline{B_{hf}} = \Delta\nu/\nu \approx 0.15]$ static hyperfine fields at the nuclei, is by itself further independent evidence for a magnetically ordered ground state of this material. The moderate value of η observed for this signal is compatible with AF order in the presence of either a small canting or significant exchange coupling with the FMM minority phase (see below). All the insulating samples of our series ($z \geq 0.6$) display both kinds of signals, with very similar features.

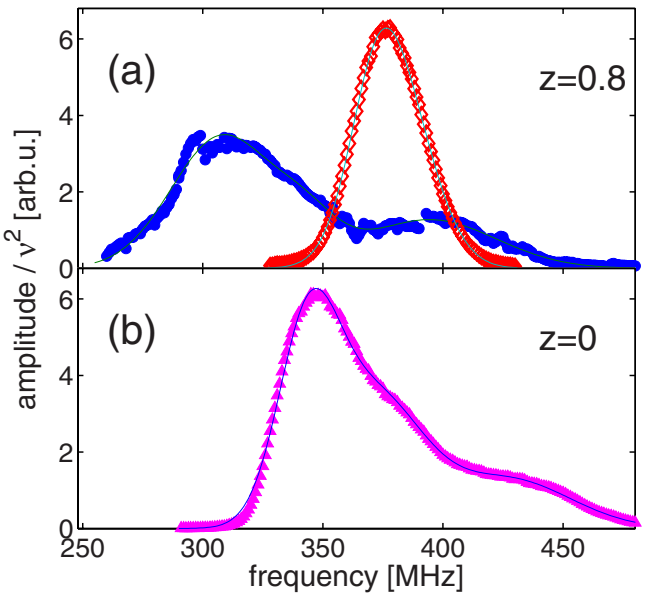

FIG. 7. (Color online) (a) $(La_{0.2}Pr_{0.8})_{1.2}Sr_{1.8}Mn_2O_7$: zero-field ^{55}Mn NMR spectra at 1.6 K of the proper (filled symbols) and impurity phases (open symbols). The plotted intensities are corrected only for the NMR spectral sensitivity $\propto \nu^2$. (b) Zero-field ^{55}Mn NMR spectrum of $La_{1.2}Sr_{1.8}Mn_2O_7$ at 5 K.

Figure 7(b) shows the ^{55}Mn spectrum of $La_{1.2}Sr_{1.8}Mn_2O_7$ ($z=0$), characterized by a large rf enhancement η. More complex spectra were reported[32] for this composition. However they were obtained on a bulk metallic single crystal, where eddy-current shielding might emphasize surface impurity phases. Our spectrum, detected on powders, consists again of two peaks [a third one, less intense, fitted at $\approx 380(4)$ MHz, is compatible with the known amount of intergrowth in this sample], which are however narrower and shifted to higher frequency with respect to the intrinsic $z \geq 0.6$ spectrum [cf. Figs. 7(a) and 7(b)]. The nuclear hyperfine spectroscopy at $z=0$ is definitely more complex than the isotropic-hyperfine single peak detected for the time-averaged Mn valence, $3+x$, in all pseudocubic DE compounds, e.g., $La_{0.67}Sr_{0.33}MnO_3$ (Ref. 31) or $La_{0.67}Ca_{0.33}MnO_3$.[33] The reason for such a difference might rely on a residual orbital order in the quasi-two-dimensional double-layer manganite, in contrast with the orbital liquid state of the metallic pseudocubic material. A detailed interpretation in terms of the orbital and magnetic structure is however outside the scope of this paper.

Here, we can simply conclude that the ^{55}Mn spectra of the double-layer DE manganite, of the insulating double-layer

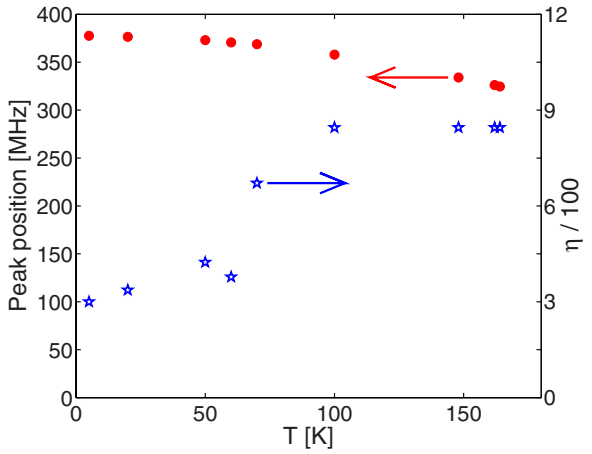

FIG. 8. (Color online) $(La_{0.4}Pr_{0.6})_{1.2}Sr_{1.8}Mn_2O_7$: mean resonance frequency (bullets) and rf enhancement (stars) of the impurity phase signal.

manganite, and of the FM intergrowth are clearly distinguishable, both in shape and enhancement. The last one in particular is very different from the former two and it identical to those recorded in the pseudocubic FMM phases. Its ZF-NMR resonance line could be followed up to approximately 170 K, above which observation of the signal was hindered by a very short spin-spin relaxation time T_2. Its mean resonance frequency $\bar{\nu}_L$, proportional to the order parameter, is plotted vs temperature in Fig. 8 for the $z=0.6$ sample. At 165 K, this quantity shows only a 15% reduction relative to its low-temperature value, indicating that the actual critical temperature of this impurity phase is significantly higher. The presence of a ZF-NMR signal well above T_N, in the same temperature range where both macroscopic magnetization and μSR detect an extrinsic response, demonstrates the coincidence of the impurity phase probed by NMR with the ferromagnetic clusters revealed above T_N by the other techniques. In addition, from the unique shape of their spectra, ^{55}Mn NMR unambiguously assigns such ferromagnetic clusters to the intergrowth of metallic $n \gg 2$ member of the R-P series, whose physical properties are probably indistinguishable from those of the pseudocubic $n=\infty$ member.

From Fig. 8, the order parameter $\bar{\nu}_L(T)$ of the impurity phase is insensitive to the Néel temperature of the double-layer material, whereas the rf enhancement factor $\eta(T)$ exhibits a steplike increase above $T_N \approx 60$ K by a factor of 3, which indicates a reduction in the effective anisotropy in the impurity phase, i.e., the magnetic softening of the ferromagnetic intergrowth at the paramagnetic transition of the host AF structure. This implies a sizable exchange coupling between the impurity and majority phases of the sample, in agreement with the large surface to volume fraction of the intergrowth. In addition it also justifies the broad peak in the ac susceptibility $\chi'(T)$ above T_N.

IV. DISCUSSION AND CONCLUSIONS

We detect an antiferromagnetic short-range-order ground state in the $z>0.5$ members of $(La_{1-z}Pr_z)_{1.2}Sr_{1.8}Mn_2O_7$. The zero-field ^{55}Mn NMR signal reveals a peak structure characteristic of the on-site hyperfine field and the small enhancement value appropriate for an insulating antiferromagnet. The drop in the muon longitudinal amplitudes below T_N and their anisotropy with respect to crystal orientation confirm a static magnetic order with the direction of the moments strongly correlated with the crystal c axis. The AF structure is further supported by the absence of a macroscopic magnetic moment and the short-range nature is deduced from the lack of a coherent μSR precession, which in this context is a sign of strong inhomogeneous relaxations.

The known spin-reorientation[28] along the c axis for $z=0.4$ is witnessed by our muon data in all $z \geq 0.4$ samples. Since the same phenomenon is observed both in the present case, where the La-Pr substitution reduces the metallic bandwidth, and in Pr-free samples, toward the border of the metallic FM phase,[34] where it is caused by a hole concentration becoming critically low, it appears as a generic feature connected to the weakening of the double-exchange interaction.

Our unsubstituted $La_{1.2}Sr_{1.8}Mn_2O_7$ crystal deserves special attention. This sample exhibits a Curie temperature of 105 K, rather lower than any previously reported T_C for this material (e.g., $T_C \approx 125$ K according to Refs. 3, 25, and 35). On the other hand, the spontaneous field at the muon of 2.2 kG detected at low temperature is in close agreement with the value reported in the literature for this material.[21] Such a comparatively low-field value corresponds to FM order with an easy magnetization axis in the ab plane. Electronic moments oriented along the c axis (as in $z=0.4$) or antiferromagnetically ordered,[21] on the contrary, would give rise in fact to much higher precession frequencies.

Therefore, the discrepancy in the Curie point in our sample cannot be due to a deviation from its nominal stoichiometry. According to the phase diagram reported in the literature,[3,35] the present value of T_C would correspond to hole concentrations x differing from the nominal value by more than 0.06, well beyond the preparation accuracy. Such large deviations in stoichiometry would also determine a significantly different magnetic structure: either canted AF, in the overdoped case, or FM with out-of-plane spin orientation,[34] such as for our $(La_{0.6}Pr_{0.4})_{1.2}Sr_{1.8}Mn_2O_7$, in the opposite case. The former circumstance is incompatible with low-temperature magnetization data, showing a saturation moment of $\approx 3.6\mu_B$ per Mn ion as appropriate for collinear ferromagnetism. The latter contrasts with the μSR spectrum, which is peculiar of a FM structure with an in-plane easy axis, hence a signature of a hole concentration close to the optimum value for maximum T_C, as pointed out above. We therefore maintain that ours is a very good Pr-free specimen of $x=0.4$ stoichiometry.

Actually, the present $La_{1.2}Sr_{1.8}Mn_2O_7$ crystal displays a true second-order phase transition characterized by a vanishing order parameter at the Curie point, as it appears in Fig. 9, where quantities proportional to the magnetic order parameter are plotted versus temperature for different samples: the μSR Larmor frequency in the present sample with the ^{139}La NMR spontaneous frequencies of two nominally identical compounds, the crystal studied by Shiotani *et al.*,[25] and the polycrystalline sample employed in our ^{55}Mn NMR measurement in Fig. 7(b),[36] respectively. All frequencies are nor-

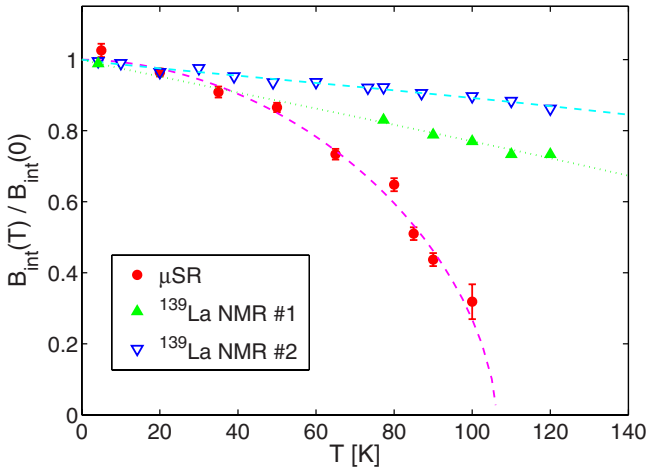

FIG. 9. (Color online) $La_{1.2}Sr_{1.8}Mn_2O_7$: normalized μSR precession frequency in the present single crystal (bullets), compared with the normalized spontaneous ^{139}La NMR frequencies at the intrabilayer site from the polycrystalline compound in Fig. 7(b) (1, filled triangles) and the crystal of Ref. 25 (2, open triangles), as a function of temperature. The reference ^{139}La frequencies at $T=0$ are 29.9 and 24.3 MHz for samples 1 and 2, respectively.

malized to their zero-temperature values. The order parameter of our crystal tends to zero for $T \rightarrow T_C$ as in a regular second-order transition, whereas the other two curves remain very high close to their transition temperature. Other samples with higher T_C were reported to exhibit magnetic transitions with strong first-order character,[37] also accompanied by marked metamagnetic properties in the PM phase, namely, the recovery of FM order in applied fields of a few teslas at tens of degrees above T_C.[1,25]

The explanation for the remarkably different behavior of our single crystal at T_C leads us to discuss the role of the intergrowths. Stacking faults in the double-layer structure with numbers of adjacent MnO_2 plane in excess of two are common in all R-P crystals of transition-metal oxides and they were actually observed in $La_{1.2}Sr_{1.8}Mn_2O_7$ by high-resolution electron microscopy.[12]

SQUID characterization reveal an amount of cubic intergrowth five times smaller in this crystal than in our polycrystalline sample in Fig. 9 and nearly a factor of 2 smaller than our other Pr-substituted crystals. We argue that the peculiar behavior of our crystal is due to its relative high purity. The double-layer manganite is exchange coupled to the intergrowths, which are known to occur as stacking faults, extended on the (001) planes and very short in the c direction. This topology maximizes their effect on the magnetic free-energy balance, possibly leading to a natural exchange-spring behavior,[38] which could result in distinct magnetic properties of the intergrowth-rich samples. It is very likely therefore that the magnetic phase transition of pure $La_{1.2}Sr_{1.8}Mn_2O_7$ is second order and takes place at a Curie point not exceeding ≈ 105 K, as in our sample, while higher T_C values and first-order-like phase transitions are both extrinsic properties, driven by the exchange coupling with the intergrowth in specimens with larger fractions of such inclusions. The same exchange coupling would also account for a metamagnetic behavior above T_C, which we actually observed in our powder sample but not in the crystal. If this scenario were confirmed, double-layered manganites samples of standard quality (i.e., impure ones) should be regarded as a natural kind of exchange-spring materials, with new physical properties arising from the interaction between the two phases.

Magnetometry and ^{55}Mn NMR provide independent and consistent evidence for the presence of intergrowths in our crystals, up to approximately 1% volume in the Pr-substituted crystals and to a few percent in our powder specimen. NMR demonstrates that these intergrowths display a ferromagnetic metallic state very close to that of the pseudocubic bulk material. In addition, NMR and susceptibility data reveal a peculiar increase in their magnetic anisotropy in coincidence with the magnetic ordering of the proper double-layer manganite phase, more evident at AF compositions thanks to the magnetic contrast between the inclusions and the host matrix. Such a magnetic hardening constitutes the proof of a strong exchange coupling between the two phases, which points to a large surface to volume ratio of the impurity domains.

Direct evidence of the FMM intergrowths comes also from the muon relaxations in Figs. 3(b) and 4, which demonstrate the static nature of the excess relaxation for $\boldsymbol{S}^0_\mu \perp \hat{c}$. Only the presence of a modest *static* local field $\boldsymbol{B}_\mu$ at the muon site may explain the quenching effect in Fig. 4. Such field cannot be understood in terms of typical paramagnetic properties, e.g., those of the $(La_{1-z}Pr_z)_{1.2}Sr_{1.8}Mn_2O_7$ matrix alone, whereas it is simply explained by distant diluted ferromagnetic impurities. However the relaxations in Fig. 3(b) indicate an unusually large anisotropy of $\boldsymbol{B}_\mu$ together with a pronounced increase in the rates for temperatures decreasing toward $T_C \approx 60$ K. Both findings are difficult to understand in terms of simple dipolar fields from distant diluted inclusions. At present we cannot offer a detailed explanation of these observations. We notice that they may indicate that the $(La_{1-z}Pr_z)_{1.2}Sr_{1.8}Mn_2O_7$ matrix is not passive in the presence of magnetized inclusions and that the two intermixed phases give rise to specific peculiar coupled magnetic properties.

In conclusion, we have demonstrated a magnetically ordered ground state in optimally hole-doped La-Pr double-layer manganites at all praseodymium concentrations and the ubiquitous presence of nanoscopic metallic pseudocubic inclusions, seemingly unavoidable with the material synthesis, which undergo independent FM ordering at higher temperature. Evidence for exchange coupling between the two phases suggests that the physical properties of double-layer manganite may be strongly affected by the intergrowths.

ACKNOWLEDGMENTS

The authors thank A. Amato for assistance and helpful discussion. Partial funding by NANOFABER and OFSPIN and the technical support of the LMU staff and of the accelerator staff of the Paul Scherrer Institute are gratefully acknowledged.

*allodi@fis.unipr.it

[1] Y. Moritomo, A. Asamitsu, H. Kuwahara, and Y. Tokura, Nature (London) **380**, 141 (1996).
[2] T. Kimura, Y. Tomioka, H. Kuwahara, A. Asamitsu, M. Tamura, and Y. Tokura, Science **274**, 1698 (1996).
[3] C. D. Ling, J. E. Millburn, J. F. Mitchell, D. N. Argyriou, J. Linton, and H. N. Bordallo, Phys. Rev. B **62**, 15096 (2000).
[4] F. Wang, A. Gukasov, F. Moussa, M. Hennion, M. Apostu, R. Suryanarayanan, and A. Revcolevschi, Phys. Rev. Lett. **91**, 047204 (2003).
[5] F. Moussa, M. Hennion, F. Wang, A. Gukasov, R. Suryanarayanan, M. Apostu, and A. Revcolevschi, Phys. Rev. Lett. **93**, 107202 (2004).
[6] M. Apostu, R. Suryanarayanan, A. Revcolevschi, H. Ogasawara, M. Matsukawa, M. Yoshizawa, and N. Kobayashi, Phys. Rev. B **64**, 012407 (2001).
[7] J. Choi, J. D. Woodward, J. L. Musfeldt, J. T. Haraldsen, X. Wei, M. Apostu, R. Suryanarayanan, and A. Revcolevschi, Phys. Rev. B **70**, 064425 (2004).
[8] M. Matsukawa, K. Akasaka, H. Noto, R. Suryanarayanan, S. Nimori, M. Apostu, A. Revcolevschi, and N. Kobayashi, Phys. Rev. B **72**, 064412 (2005).
[9] Z. Sun, J. F. Douglas, A. V. Fedorov, Y.-D. Chuang, H. Zheng, J. F. Mitchell, and D. S. Dessau, Nat. Phys. **3**, 248 (2007).
[10] P. Wagner, I. Gordon, V. V. Moshchalkov, Y. Bruynseraede, M. Apostu, R. Suryanarayanan, and A. Revcolevschi, Europhys. Lett. **58**, 285 (2002).
[11] P. V. Patanjali, P. Theule, Z. Zhai, N. Hakim, S. Sridhar, R. Suryanarayanan, M. Apostu, G. Dhalenne, and A. Revcolevschi, Phys. Rev. B **60**, 9268 (1999).
[12] S. D. Bader, R. M. Osgood III, D. J. Miller, J. F. Mitchell, and J. S. Jiang Osgood, J. Appl. Phys. **83**, 6385 (1998).
[13] M. Matsukawa, M. Narita, T. Nishimura, M. Yoshizawa, M. Apostu, R. Suryanarayanan, A. Revcolevschi, K. Itoh, and N. Kobayashi, Phys. Rev. B **67**, 104433 (2003).
[14] G. Allodi, A. Banderini, R. De Renzi, and C. Vignali, Rev. Sci. Instrum. **76**, 083911 (2005).
[15] A. J. Freeman and R. E. Watson, *Hyperfine Interactions in Magnetic Materials and Magnetism*, edited by G. T. Rado and H. Suhl (Academic, New York, 1965), Vol. II, Pt. A.
[16] T. Kubo, A. Hirai, and H. Abe, J. Phys. Soc. Jpn. **26**, 1094 (1969).
[17] P. A. Algarabel, J. M. De Teresa, J. Blasco, M. R. Ibarra, Cz. Kapusta, M. Sikora, D. Zajac, P. C. Riedi, and C. Ritter, Phys. Rev. B **67**, 134402 (2003).
[18] A. M. Portis and R. H. Linquist, *Nuclear Resonance in Ferromagnetic Materials and Magnetism*, edited by G. T. Rado and H. Suhl (Academic, New York, 1965), Vol. II, Pt. A.
[19] M. A. Turov and M. P. Petrov, *Nuclear Magnetic Resonance in Ferro- and Antiferromagnets* (Halsted, New York, 1972).
[20] A. Schenck, *Muon Spin Rotation: Principles and Applications in Solid State Physics* (Hilger, Bristol, 1985).
[21] A. I. Coldea, S. J. Blundell, C. A. Steer, J. F. Mitchell, and F. L. Pratt, Phys. Rev. Lett. **89**, 277601 (2002).
[22] R. H. Heffner, L. P. Le, M. F. Hundley, J. J. Neumeier, G. M. Luke, K. Kojima, B. Nachumi, Y. J. Uemura, D. E. MacLaughlin, and S.-W. Cheong, Phys. Rev. Lett. **77**, 1869 (1996).
[23] M. C. Guidi, G. Allodi, R. De Renzi, G. Guidi, M. Hennion, L. Pinsard, and A. Amato, Phys. Rev. B **64**, 064414 (2001).
[24] C. Baumann, G. Allodi, B. Buchner, R. De Renzi, P. Reutler, and A. Revcolevschi, Physica B (Amsterdam) **326**, 505 (2003).
[25] Y. Shiotani, J. L. Sarrao, and Guo-qing Zheng, Phys. Rev. Lett. **96**, 057203 (2006).
[26] M. K. Gubkin, A. V. Zalesskii, V. G. Krivenko, T. M. Perekalina, K. A. Khimich, and V. A. Chubarenko, JETP Lett. **60**, 56 (1994).
[27] C. P. Adams, J. W. Lynn, V. N. Smolyaninova, A. Biswas, R. L. Greene, W. Ratcliff, S. W. Cheong, Y. M. Mukovskii, and D. A. Shulyatev, Phys. Rev. B **70**, 134414 (2004).
[28] A. Vasil'ev, T. Voloshok, M. Apostu, R. Suryanarayanan, and A. Revcolevschi, JETP Lett. **73**, 630 (2001).
[29] R. De Renzi, G. Allodi, G. Amoretti, M. Cestelli Guidi, S. Fanesi, G. Guidi, F. Licci, A. Caneiro, F. Prado, R. Sanchez, S. Oseroff, and A. Amato, Physica B (Amsterdam) **289-290**, 85 (2000).
[30] R. H. Heffner, D. E. MacLaughlin, G. J. Nieuwenhuys, T. Kimura, G. M. Luke, Y. Tokura, and Y. J. Uemura, Phys. Rev. Lett. **81**, 1706 (1998).
[31] A. A. Sidorenko, G. Allodi, R. De Renzi, G. Balestrino, and M. Angeloni, Phys. Rev. B **73**, 054406 (2006).
[32] K. Shimizu, M. Velazquez, J. P. Renard, and A. Revcolevschi, J. Phys. Soc. Jpn. **72**, 793 (2003).
[33] M. Bibes, Ll. Balcells, S. Valencia, J. S. Fontcuberta, M. Wojcik, E. Jedryka, and S. Nadolski, Phys. Rev. Lett. **87**, 067210 (2001).
[34] J. F. Mitchell, D. N. Argyriou, A. Berger, K. E. Gray, R. Osborne, and U. Welp, J. Phys. Chem. B **105**, 10731 (2001).
[35] M. Kubota, H. Fujioka, K. Hirota, K. Ohoyama, Y. Moritomo, H. Yoshizawa, and Y. Endoh, J. Phys. Soc. Jpn. **69**, 1606 (2000).
[36] G. Allodi and R. De Renzi (unpublished).
[37] A. Berger, J. F. Mitchell, D. J. Miller, and S. D. Bader, J. Appl. Phys. **89**, 6851 (2001).
[38] G. Asti, M. Solzi, M. Ghidini, and F. M. Neri, Phys. Rev. B **69**, 174401 (2004).
[39] Mass rf susceptibilities are calculated from Eq. (1) by assuming filling factors f on the order of 0.3–0.5 and neglecting the demagnetization term $N4\pi\chi_{\mathrm{rf}}$.
[40] The large uncertainty in the amplitude ratio follows from the extrapolation of the spin-echo amplitudes at $\tau=0$ in the presence of short T_2 (especially for the AF signal), as well as from the inhomogeneity of η, which prevents simultaneous optimum excitation of all nuclei.